Supplementary Information

Chemical activation of forage grass-derived biochar for treatment of aqueous antibiotic sulfamethoxazole

Shengquan Zeng[†], Eunsung Kan[†,‡,*]

Affiliations:

[†]Department of Biological and Agricultural Engineering & Texas A&M AgriLife Research Center, Texas A&M University, TX 76401, USA

[‡]Department of Wildlife, Sustainability, and Ecosystem Sciences, Tarleton State University, TX 76401, USA.

[*] **Corresponding author. Tel.: +1-254-968-4144; fax: +1-254-968-3759.**

E-mail address: Eunsung.Kan@ag.tamu.edu

Characterization of biochars

Elemental compositions of all BCs were evaluated by an elemental analyzer (PerkinElmer 2400 series II, MA, USA) (Robert Microlit Lab, NJ, USA). According to ASTM standard D7582-10 [1], the proximate analysis was used to evaluate the contents of fixed carbon, volatile carbon and ash in BCs. Brunauer-Emmett-Teller (BET) surface area was evaluated with an apparatus at 77 K based on the measurements relating to N_2 sorption (Particle Technology Lab, Downers Grove, USA). Functional groups in BCs were evaluated by FT-IR spectra, which were recorded between 400 and 4000 cm^{-1} using a FT-IR spectrometer (Bruker Optik GmbH, Ettlingen, Germany). To evaluate the crystallographic structures at the surface of BCs, an X-ray diffractometer (MiniFlex II, DE, USA) was used to assess the X-ray diffraction (XRD) patterns of BCs operating at 30 kV and 15 mA with a step size of 0.02° (2θ). The pH of zero point charges (pH_{PZC}) of BCs were determined as described by the previous study [2]. Briefly, 0.01 g BC was added into 50 mL of NaCl solution (0.01 M), the initial pH of which was adjusted ranged from 3.0 to 10.0 using 0.1 M HCl or NaOH solution. After 2-day incubation at 20 °C and 150 rpm, the pH_{PZC} of BCs were obtained based on the ΔpH (final – initial pH) = 0.

Data analysis

In this study, the determination coefficients (R^2) and the sum of squared error (SSE) were used to determine which model best fit the experimental data:

$$R^2 = 1 - \frac{\Sigma(Q_{exp} - Q_{cal})^2}{\Sigma(Q_{exp} - Q_{mean})^2} \qquad (1)$$

$$\mathrm{SSE} = \sqrt{\frac{\Sigma(Q_{exp} - Q_{cal})^2}{N}} \qquad (2)$$

where Q_{exp}, Q_{cal} and Q_{mean} are the experimental value, calculated value and mean of experimental value, respectively, and N is the number of measurements.

Table S1. Maximum adsorption capacity (Q_m) of various adsorbents for sulfamethoxazole

Adsorbents	Surface area (m^2/g)	Q_m (mg/g)	Reference
Carbon nanotubes	382	71.8[a]	[3]
Graphene Oxide	-	240[a]	[4]
Bamboo BC	1.12	88.1[a]	[5]
Alfalfa BC	405	90.4[a]	[6]
Commercial AC (ChemViron Carbon)	848	118[a]	[7]
Pine Sawdust BC	125	13.8[a]	[8]
Digested bagasse BC	17.66	54.38[a]	[9]
R-BC	1.67	23.56[b]	In this study
BC800	85.82	26.68[b]	In this study
A-BC	1999.59	456.11[b]	In this study
Commercial AC (Calgon F400)	816.3[11]	312.14[b]	[10]
Commercial AC (Darco® G-60)	933[12]	328.83[b]	[10]
Commercial AC (Norit® GAC)	1200[13]	377.5[b]	[10]

BC: Biochar

AC: Activated Carbon

R-BC: Raw biochar produced at 300 °C (in this study)

BC800: Biochar produced at 800 °C (in this study)

A-BC: Activated biochar (in this study)

[a]Derived from isotherm model

[b]Derived from experimental data

Table S2. Characteristics of various activated carbons.

Adsorbents	Surface area (m^2/g)	Elemental compositions				O/C	H/C	Ash (%)	Reference
		C	H	O	N				
A-BC (This study)	1991.6	81.22	0.84	7.42	0.83	0.07	0.12	9.46	
Commercial activated carbon (Calgon F400)	1102	82.85	0.93	9.27	0.55	0.08	0.13	5.40	[14]
Commercial activated carbon (Alphacarbo)	525.3	78.62	1.28	19.77	0.33	0.19	0.20	5.03	[15]
Commercial activated carbon (Steam activated coconut shell)	1138	90.1	0.2	9.0	-	0.07	0.03	0.4	[16]
Commercial activated carbon (H_3PO_4 activated wood)	1515	64.8	2.4	19.5	-	0.23	0.44	1.1	[16]
Activated carbon (K_2CO_3 activated tobacco residue)	1634	55.25	0.22	45.38	0.95	0.62	0.05	-	[17]
Activated carbon (KOH activated tobacco residue)	1474	49.40	0.28	48.80	1.52	0.74	0.07	-	[17]
Activated carbon (Steam activated beet pulp)	821	77.9	0.9	7.0	0.6	0.07	0.14	13.6	[16]
Activated carbon (Steam activated peanut shell)	829	91.2	0.8	6.0	0.2	0.05	0.11	1.3	[16]

Table S3. Physicochemical characteristics of sulfamethoxazole (SMX) [10, 18].

Molecular structure	**Formula**	**Molecular weight**	**Solubility[a]**	**pK_a**
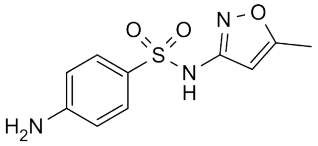	$C_{10}H_{11}N_3O_3S$	253.28	0.37 g/L	$pK_1 = 1.6$ $pK_2 = 5.7$

[a] At ambient temperature

Table S4. Calculated sorption coefficients for three SMX species on A-BC at pH 1-12.

pH	K_d	K_d^+	K_d^0	K_d^-
1	6402	7357	2597	1000
2	7762	4237	9167	1002
3	8229	1294	8519	1016
4	8139	1025	8306	1148
5	7145	998	8090	2423
6	6199	995	4105	7248
7	5478	994	1232	5690
8	5356	992	1020	5378
9	5561	992	1000	5563
10	2934	991	997	2934

Table S5. Contribution of different SMX species to the overall sorption on A-BC.

pH	Contribution percent (%)		
	SMX^+	SMX^0	SMX^-
1	91.86	8.14	<0.01
2	15.54	84.46	<0.01
3	0.60	99.38	0.02
4	0.05	99.68	0.28
5	<0.01	94.35	5.64
6	<0.01	22.11	77.89
7	<0.01	1.07	98.93
8	<0.01	0.10	99.90
9	<0.01	<0.01	99.99
10	<0.01	<0.01	99.99

*Contribution percentage was calculated by $K_d^+\alpha^+/K_d$ for SMX^+, $K_d^0\alpha^0/K_d$ for SMX^0, and $K_d^-\alpha^-/K_d$ for SMX^-.

Table S6. Characteristics of lagoon wastewater from dairy farm (Stephenville, TX, USA).

COD (ppm)	1050
Total N (ppm)	460
Total P (ppm)	57
Total K (ppm)	676
Total Ca (ppm)	227
Total Mg (ppm)	157
Total Na (ppm)	277

Table S7. Adsorption isotherm, kinetic, and thermodynamic models used in this study.

Models	Names and Equations
Kinetics	Pseudo-first order: $Q_t = Q_e(1 - exp(-K_1 t))$
	Pseudo-second order: $Q_t = \frac{K_2 Q_e^2 t}{1 + K_2 Q_e t}$
	Elovich: $Q_t = \left(\frac{1}{b}\right) lnab + \left(\frac{1}{b}\right) lnt,\ t_0 = \frac{1}{ab}$
	Intra-particle diffusion: $Q_t = K_i\sqrt{t} + C_i$
	Film diffusion(Boyd equation): $B_t = -\ln\left(1 - \frac{Q_t}{Q_e}\right) - 0.4977$
Isotherm	Freundlich isotherm: $Q_e = K_f C_e^{\frac{1}{nf}}$
	Langmuir isotherm: $Q_e = \frac{Q_m K_L C_e}{1 + K_L C_e}, R_L = \frac{1}{1 + K_L C_0}$
	Temkin isotherm: $Q_e = \frac{RT}{b_T} \ln\,(K_T C_e)$
	Dubinin-Radushkevich: $Q_e = K_{DR} exp(-B_D \varepsilon_D^2)$ $\varepsilon_D = RTln\left(1 + \frac{1}{C_e}\right); E = \frac{1}{\sqrt{2B_D}}$
Thermodynamics	$K_d = \frac{Q_e}{C_e}$
	$\Delta G^o = -\mathrm{RT}\ln(K_d)$
	$\ln\,(K_d) = -\frac{\Delta G^o}{RT} = \frac{\Delta S^o}{R} - \frac{\Delta H^o}{RT}$

Q_t: adsorption capacity (mg g^{-1}) at time t (min).
Q_e: adsorption capacity (mg g^{-1}) at equilibrium time.
K_1: adsorption rate constant of Pseudo-first order (min^{-1}).
K_2: adsorption rate constant of Pseudo-second order (min^{-1}).
a: initial adsorption rate (mg/g.min).
b: desorption constant (g/mg).
K_i: Intra-particle diffusion rate constant (mg $min^{0.5}$ g^{-1}).
C_i: the intercept reflecting the boundary layer thickness.
B_t: Boyd constant, predicting the adsorption rate-limiting step.
C_e: equilibrium concentration at liquid phase (mg L^{-1}).
K_f: distribution coefficient (mg/g), it implies that the energy of adsorption on a homogeneous surface is independent of surface coverage.
$1/n_f$: related to the surface heterogeneity, more close to zero means more heterogeneous surface.
Q_m: maximum adsorption capacity (mg/g) from monolayer adsorption.
K_L: Langmuir constant (L/g) describing the adsorption/desorption equilibrium for each reactant in

contact with a surface.

R_L: separation constant; the adsorption is irreversible $R_L=0$, favorable $0<R_L<1$, linear $R_L=1$, and unfavorable $R_L>1$.

R: universal gas constant (8.314 J $mol^{-1}K^{-1}$).

T: temperature in terms of Kelvin.

b_T: Temkin constant (J/mol), defined as variation of adsorption energy; the adsorption is exothermic ($b_T>1$) or endothermic ($b_T<1$)

K_T: equilibrium bond constant related to the maximum energy of bond (mg/L).

K_{DR}: adsorption capacity (mg/g), multilayer adsorption

B_D: mean free energy of sorption (mol^2/kJ^2).

E: bonding energy of the ion-exchange mechanism (kJ/mol).

ε_D: adsorption potential.

ΔH^o = standard enthalpy change.

ΔS^o = standard entropy change.

ΔG^o = standard Gibbs free energy change.

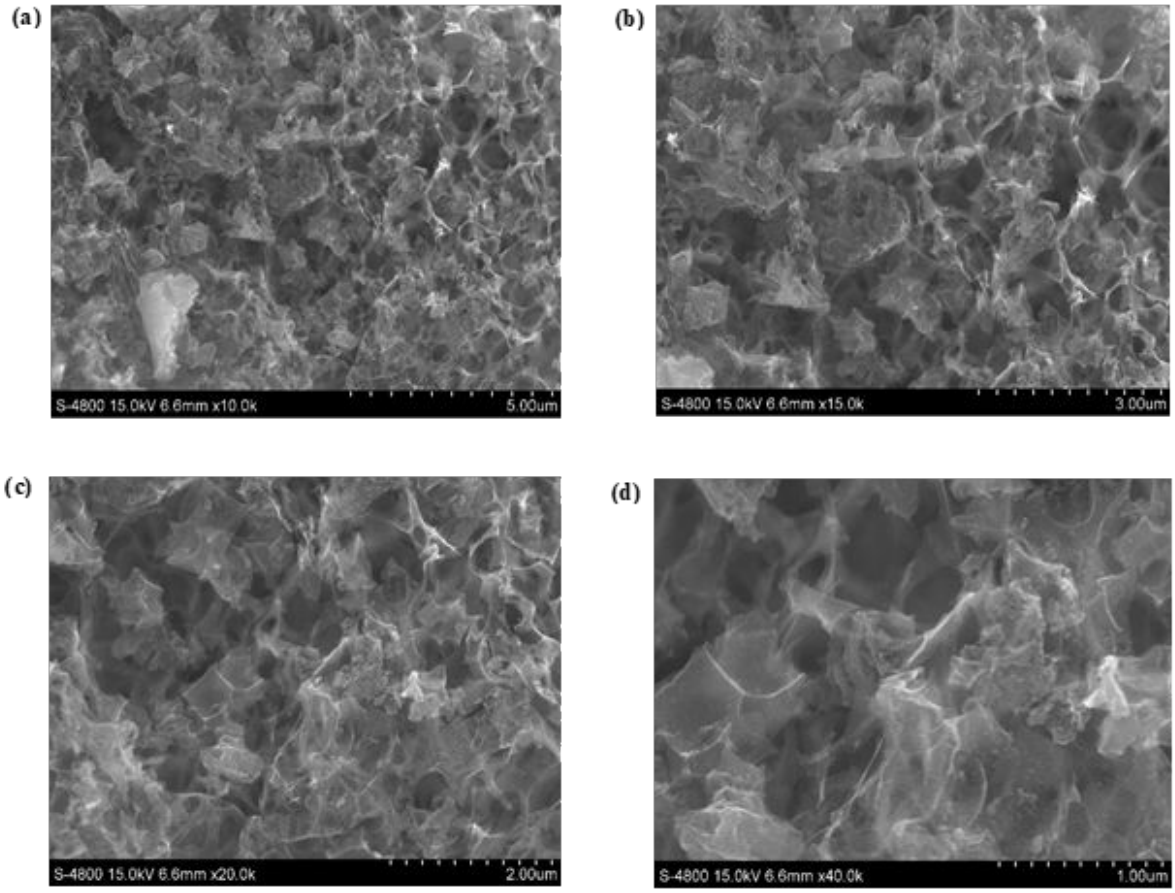

Figure S1. SEM images of A-BC at various magnifications (a:10,000; b:15,000; c:20,000; d:40,000)

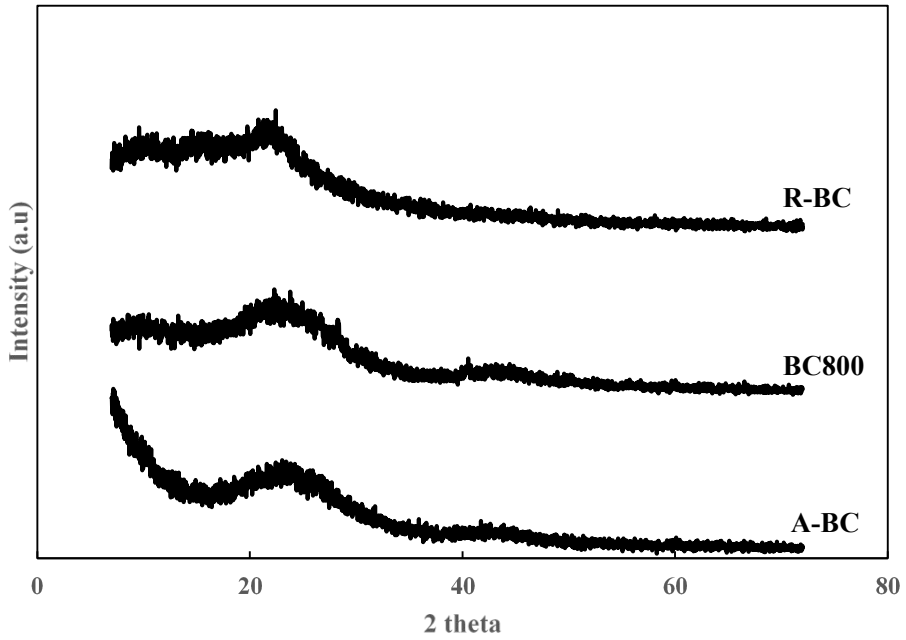

Figure S2. XRD pattern of all BCs.

R-BC: Raw biochar produced at 300 °C

BC800: Biochar produced at 800 °C

A-BC: Activated biochar

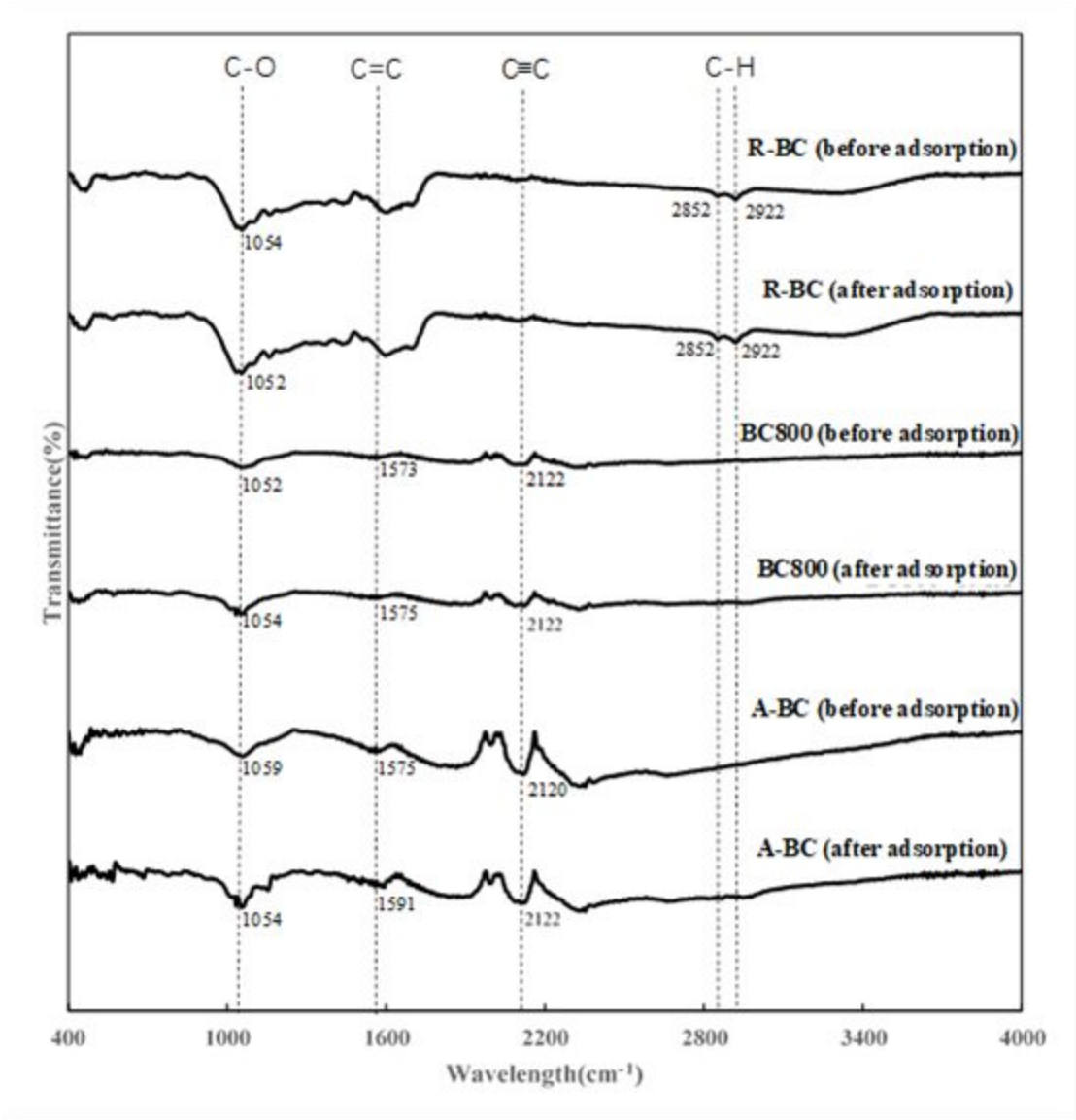

Figure S3. FT-IR spectrum of all BCs before and after SMX adsorption.

R-BC: Raw biochar produced at 300 °C

BC800: Biochar produced at 800 °C

A-BC: Activated biochar

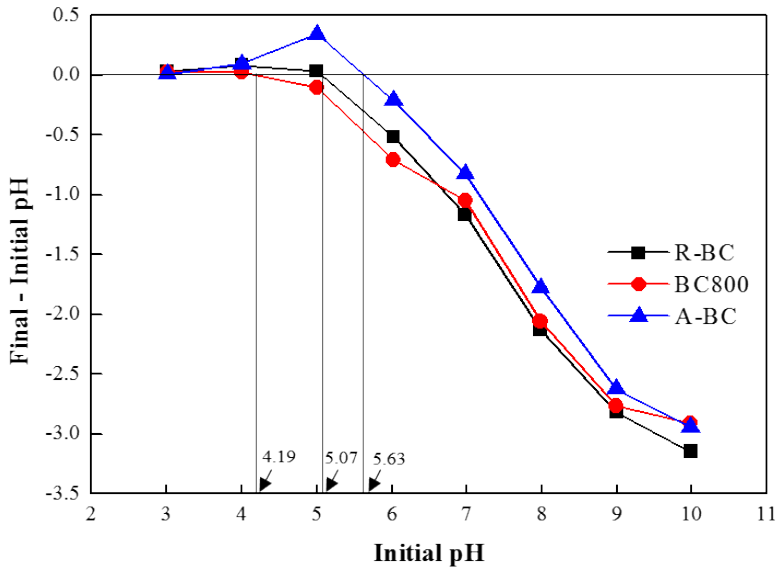

Figure S4. The pH_{PZC} of all BCs.

R-BC: Raw biochar produced at 300 °C

BC800: Biochar produced at 800 °C

A-BC: Activated biochar

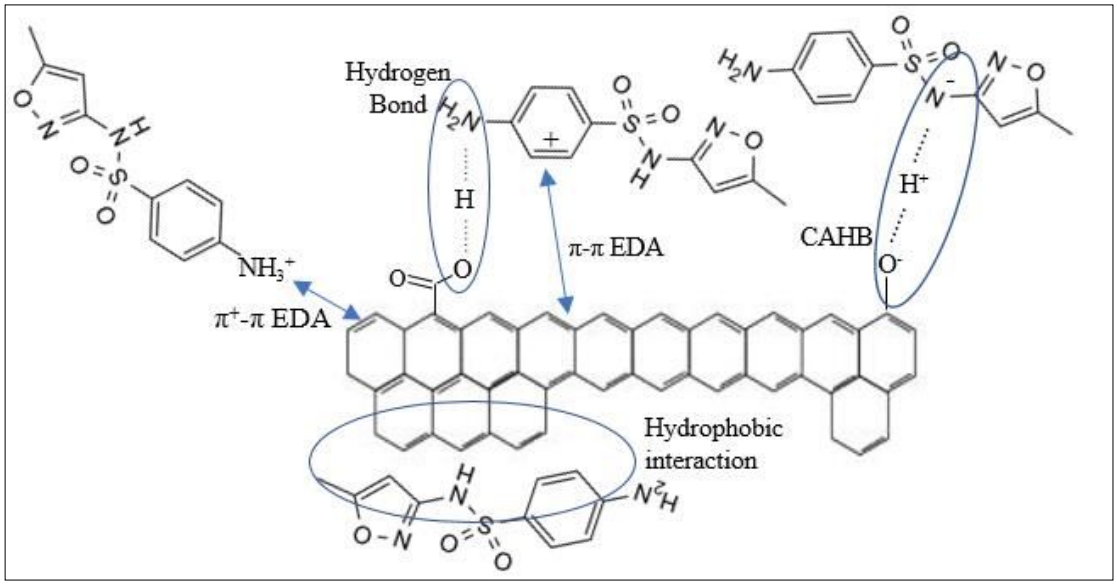

Figure S5. Proposed mechanisms for SMX adsorption on A-BC.

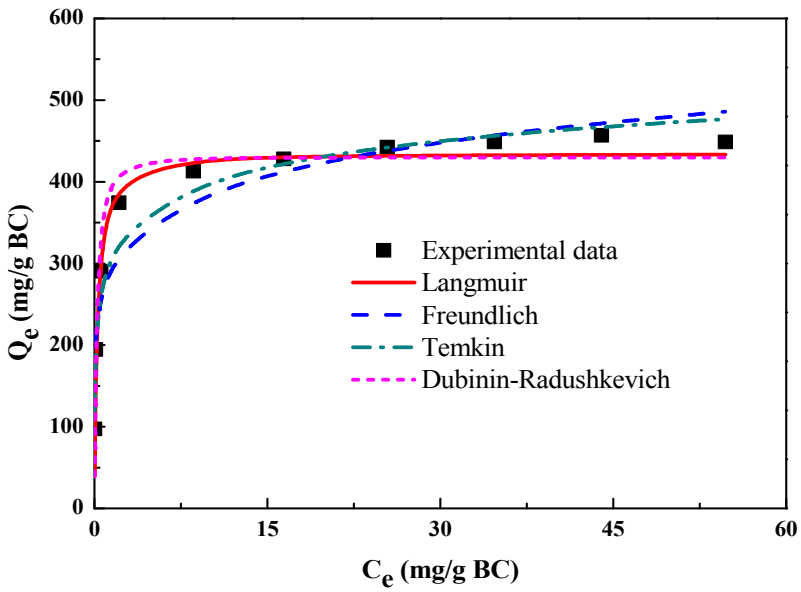

Figure S6. Adsorption isotherm of SMX on A-BC.

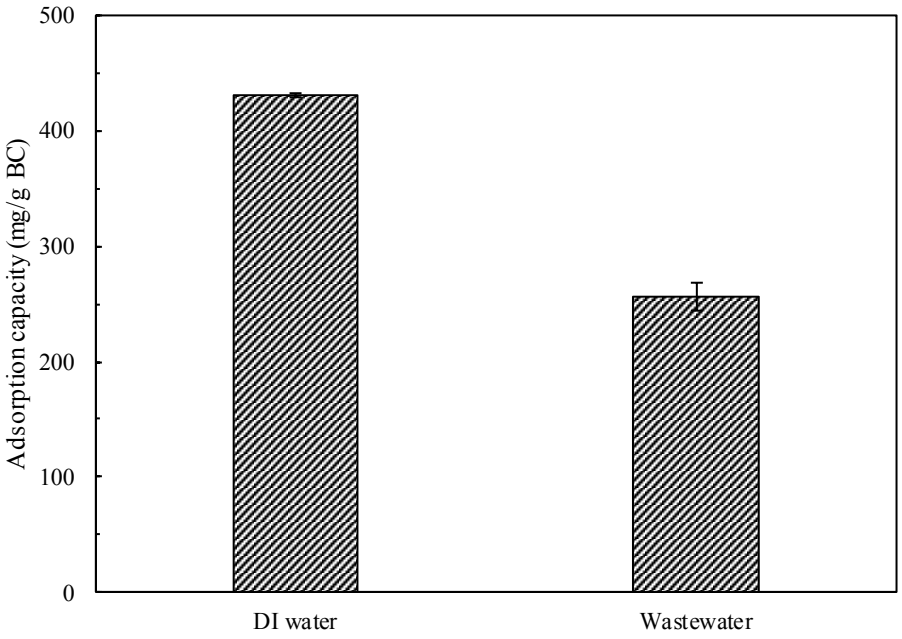

Figure S7. Adsorption of SMX onto A-BC in DI water and real wastewater. Adsorption conditions: 0.01 g of A-BC, initial pH of 6, 100 mL of 100 mg/L SMX, and 3 day.

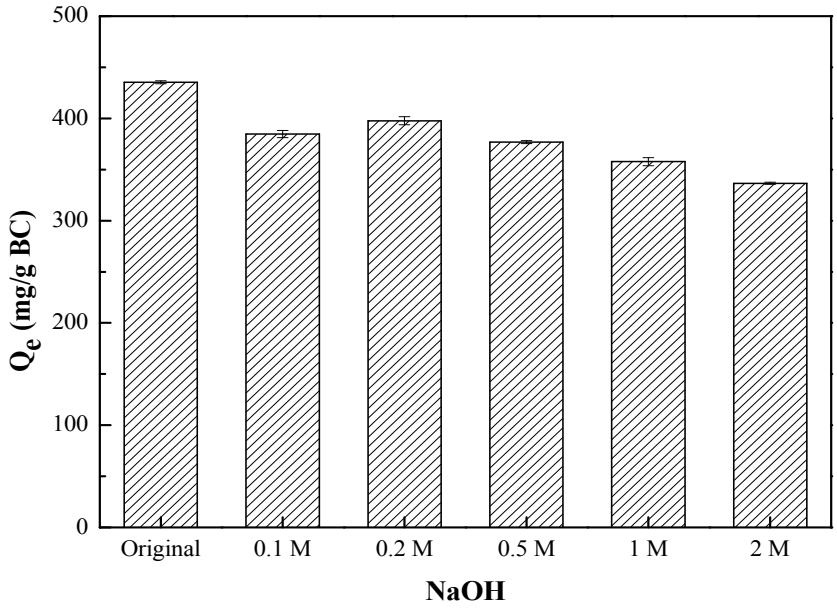

Figure S8. Effect of different NaOH concentration on the regeneration of A-BC.

References

(1) ASTM, A., D7582–10. Standard Test Methods for Proximate Analysis of Coal and Coke by Macro Thermogravimetric Analysis. *Annual Book of ASTM Standards. American Society for Testing and Materials, West Conshohocken, PA* **2010**.

(2) Jang, H. M.; Yoo, S.; Choi, Y. K.; Park, S.; Kan, E. Adsorption isotherm, kinetic modeling and mechanism of tetracycline on Pinus taeda-derived activated biochar. *Bioresour. Technol.* **2018,** *259*, 24-31.

(3) Zhao, H.; Liu, X.; Cao, Z.; Zhan, Y.; Shi, X.; Yang, Y.; Zhou, J.; Xu, J. Adsorption behavior and mechanism of chloramphenicols, sulfonamides, and non-antibiotic pharmaceuticals on multi-walled carbon nanotubes. *J. Hazard. Mater.* **2016,** *310*, 235-245.

(4) Chen, H.; Gao, B.; Li, H. Removal of sulfamethoxazole and ciprofloxacin from aqueous solutions by graphene oxide. *J. Hazard. Mater.* **2015,** *282*, 201-207.

(5) Ahmed, M. B.; Zhou, J. L.; Ngo, H. H.; Guo, W.; Johir, M. A. H.; Sornalingam, K. Single and competitive sorption properties and mechanism of functionalized biochar for removing sulfonamide antibiotics from water. *Chem. Eng. J.* **2017,** *311*, 348-358.

(6) Choi, Y. K.; Kan, E. Effects of pyrolysis temperature on the physicochemical properties of alfalfa-derived biochar for the adsorption of bisphenol A and sulfamethoxazole in water. *Chemosphere* **2019,** *218*, 741-748.

(7) Calisto, V.; Ferreira, C. I.; Oliveira, J. A.; Otero, M.; Esteves, V. I. Adsorptive removal of pharmaceuticals from water by commercial and waste-based carbons. *J. Environ. Manage.* **2015,** *152*, 83-90.

(8) Reguyal, F.; Sarmah, A. K.; Gao, W. Synthesis of magnetic biochar from pine sawdust via oxidative hydrolysis of $FeCl_2$ for the removal sulfamethoxazole from aqueous solution. *J. Hazard. Mater.* **2017,** *321*, 868-878.

(9) Yao, Y.; Zhang, Y.; Gao, B.; Chen, R.; Wu, F. Removal of sulfamethoxazole (SMX) and sulfapyridine (SPY) from aqueous solutions by biochars derived from anaerobically digested bagasse. *Environ. Sci. Pollut. Res.* **2018,** *25* (26), 25659-25667.

(10) Jang, H. M.; Yoo, S.; Park, S.; Kan, E. Engineered biochar from pine wood: Characterization and potential application for removal of sulfamethoxazole in water. *Environ.Eng. Res.* **2018,** *24* (4), 608-617.

(11) Gauden, P. A.; Szmechtig-Gauden, E.; Rychlicki, G.; Duber, S.; Garbacz, J. K.; Buczkowski, R. Changes of the porous structure of activated carbons applied in a filter bed pilot operation. *J. Colloid Interface Sci.* **2006,** *295* (2), 327-347.

(12) Oliveira, L. C.; Rios, R. V.; Fabris, J. D.; Garg, V.; Sapag, K.; Lago, R. M. Activated carbon/iron oxide magnetic composites for the adsorption of contaminants in water. *Carbon* **2002,** *40* (12), 2177-2183.

(13) Gicheva, G.; Yordanov, G. Removal of citrate-coated silver nanoparticles from aqueous dispersions by using activated carbon. *Colloid. Surface. A* **2013,** *431*, 51-59.

(14) Jang, H. M.; Kan, E. A novel hay-derived biochar for removal of tetracyclines in water. *Bioresour. Technol.* **2019,** *274*, 162-172.

(15) Pego, M. F.; Bianchi, M. L.; Carvalho, J. A.; Veiga, T. R. Surface modification of activated carbon by corona treatment. *An. Acad. Bras. Ciênc.* **2019,** *91* (1).

(16) Torres-Pérez, J.; Gérente, C.; Andrès, Y. Sustainable activated carbons from agricultural residues dedicated to antibiotic removal by adsorption. *Chin. J. Chem. Eng.* **2012,** *20* (3), 524-529.

(17) Kilic, M.; Apaydin-Varol, E.; Pütün, A. E. Adsorptive removal of phenol from aqueous solutions on activated carbon prepared from tobacco residues: equilibrium, kinetics and thermodynamics. *J. Hazard. Mater.* **2011,** *189* (1-2), 397-403.

(18) MartÍnez, F.; GÓmez, A. Estimation of the solubility of sulfonamides in aqueous media from partition

coefficients and entropies of fusion. *Phys. Chem. Liq.* **2002,** *40* (4), 411-420.